Published in final edited form as:
Neuroimage. 2008 January 1; 39(1): 248–260.

BOLD Study of Stimulation-Induced Neural Activity and Resting-State Connectivity in Medetomidine-Sedated Rat

Fuqiang Zhao, **Tiejun Zhao**, **Lei Zhou**, **Qiulin Wu**, and **Xiaoping Hu**
Wallace H. Coulter Department of Biomedical Engineering, Georgia Institute of Technology and Emory University, 101 Woodruff Circle, Suite 2001, Atlanta, GA 30322, USA.

Abstract

Functional magnetic resonance imaging (fMRI) in anesthetized-animals is critical in studying the mechanisms of fMRI and investigating animal models of various diseases. Medetomidine was recently introduced as an independent anesthesia for longitudinal (survival) fMRI studies in rats. Since stimulation-induced fMRI signal is anesthesia-dependent and its characteristics in rats under medetomidine are not fully elucidated, the blood oxygenation level dependent (BOLD) fMRI response to electrical forepaw stimulation under medetomidine was systematically investigated at 9.4 T. Robust activations in contralateral primary somatosensory cortex (SI) and thalamus were observed and peaked at the stimulus frequency of 9 Hz. The response in SI saturates at the stimulus strength of 4 mA while the response in thalamus monotonically increases. In addition to fMRI data acquired with the forepaw stimulation, data were also acquired during the resting-state to investigate the synchronization of low frequency fluctuations (LFF) in the BOLD signal (<0.08 Hz) in different brain regions. LFF during resting-state have been observed to be synchronized between functionally related brain regions in human subjects while its origin is not fully understood. LFF have not been extensively studied or widely reported in anesthetized-animals. In our data, synchronized LFF of BOLD signals are found in clustered, bilaterally symmetric regions, including SI and caudate putamen and the magnitude of the LFF is ~1.5%, comparable to the stimulation-induced BOLD signals. Similar to resting-state data reported in human subjects, LFF in rats under medetomidine likely reflect functional connectivity of these brain regions.

Keywords

fMRI; functional connectivity; medetomidine; somatosensory pathway; low frequency fluctuation (LFF)

INTRODUCTION

Functional magnetic resonance imaging (fMRI) (Ogawa and Lee, 1990) has been widely used to study the neural basis of perception, cognition, and emotion. Such studies have traditionally focused on brain regions showing task-related changes in neural activity. Neural activation leads to a series of physiological events in the brain, including localized increase in cerebral blood flow (CBF), cerebral blood volume (CBV), and cerebral metabolic rate of oxygen ($CMRO_2$), which are collectively termed “the hemodynamic response.” These hemodynamic events cause a change in the venous blood oxygen level, which can be detected by the blood

Corresponding author: Xiaoping Hu, Biomedical Imaging Technology Center, 101 Woodruff Circle, Suite 2001, Atlanta, GA 30322, e-mail: xhu@bme.gatech.edu, phone: 404-712-2615, fax: 404-712-2707.

oxygen level dependent (BOLD) fMRI technique (Ogawa et al., 1990; Ogawa et al., 1993). Since the coupling between the hemodynamic response and the neural activity is similar between awake humans and anesthetized animals and invasive techniques such as local field potential and single unit recordings can be performed simultaneously during fMRI study in animals, fMRI in anesthetized animals has been extensively used in studying the mechanism of fMRI and non-cognition related brain functions (Logothetis et al., 2001; Ogawa et al., 2000; Shmuel et al., 2006).

Rat fMRI of somatosensory pathway in response to electrical stimulation of paw is an interesting animal model for fMRI because of the wealth of existing fMRI data (Duong et al., 2000; Keilholz et al., 2004; Lee et al., 2002; Silva and Koretsky, 2002) and data from other modalities such as optical imaging and electrophysiological recording (Masamoto et al., 2007; Sheth et al., 2005). However, to date, most rat fMRI studies have been performed in α-chloralose anesthetized rats requiring the animal to be euthanized after the experiment due to invasive intubation and catheterization. It is desirable to establish a protocol that can monitor brain plasticity and functional recovery after brain injury by fMRI (Dijkhuizen et al., 2003) in a longitudinal manner with a survival experimental protocol.

In addition to studying task-related neural activation, it is also possible to use fMRI to study the brain at rest. Studies in human subjects have shown that low frequency fluctuations (LFF) of the BOLD signal are temporally synchronized between functionally related brain regions, including motor, auditory, visual, sensorimotor systems, and even subcortical nucleus (Biswal et al., 1995; Biswal et al., 1997; Damoiseaux et al., 2006; Greicius et al., 2003; Lowe et al., 1998; Stein et al., 2000). Thus, the synchronized LFF are believed to reflect functional connectivity: a measure of spatio-temporal correlations between spatially distinct brain regions. Although the exact origin of the synchronized LFF of BOLD has not been fully elucidated and some studies even suggest that the synchronized LFF of BOLD signal in humans reflect changes in underlying brain physiology independent of neural activation (Kiviniemi et al., 2000), resting connectivity based on synchronized LFF is widely used. In fact, the synchronized LFF is used not only to map the resting-state neural networks and the strength of the synchronization (correlation) but also as an index to evaluate pathological conditions such as Alzheimer's disease (Li et al., 2002) or multiple sclerosis (Lowe et al., 2002) and the effects of drugs such as cocaine (Li et al., 2000), anesthetic agents (Anand et al., 2005; Peltier et al., 2006) and antidepressant (Anand et al., 2005). In animal models, LFF in the neuronal electrical activities have been observed by transcortical electroencephalographic (EEG) technique (Allers et al., 2002), by local field potential (Leopold et al., 2003) and by single unit recording (Ruskin et al., 2003) without the use of general anesthesia but are greatly reduced by anesthesia (Ruskin et al., 1999). The LFF's dependence on anesthesia makes the detection and study of the LFF of BOLD signal difficult in animal models. The ability to detect synchronized LFF of BOLD signal in animal models will open up new avenues for further investigation of LFF and for examining it under various physiological and pathological conditions.

Medetomidine (domitor) is an α_2 adrenoreceptor agonist which can provide sedation and anxiolysis, analgesia and some muscle relaxation (Lukasik and Gillies, 2003). It is generally used as an adjuvant to reduce anesthetic requirements to tracheal intubation and surgical stimuli (Bol et al., 1999). It was first used in rat fMRI as an independent anesthesia by Weber and colleagues (Weber et al., 2006). Since it is administered subcutaneously requiring no catheterization, and the animal is maintained in a free breathing state requiring no intubation, a medetomidine anesthesia protocol can be used for longitudinal (survival) fMRI studies. Although the feasibility to perform longitudinal fMRI by medetomidine in rats has been previously demonstrated (Weber et al., 2006), the characteristics of the BOLD response under medetomidine have not been fully investigated. It has been previously reported that the BOLD

response depends on the anesthetic agent used (Masamoto et al., 2007; Silva et al., 1999). Therefore, we investigated the dependence of the BOLD response to electrical forepaw stimulation under medetomidine on the frequency and the strength of the stimulus and subsequently, with optimized stimulus parameters, investigated the spatial and temporal characteristics of the stimulation-induced BOLD fMRI in the somatosensory network. In the study by Weber and colleagues, the dose that was chosen provided "a sedation level adequate for reliable fMRI experiments" (Weber et al., 2006). Using the suggested dose of medetomidine, the animal is under sedation rather than full anesthesia, and synchronized LFF of BOLD signal may be detected. Therefore, in addition to performing the BOLD study of stimulation-induced neural activity, BOLD data was also acquired during the resting-state to investigate the possibility of detecting and the characteristics of resting-state connectivity under *medetomidine-sedation*. Combining somatosensory task-related fMRI with the functional connectivity during resting-state can provide complementary information for investigating the relevance between the somatosensory pathway and the resting-state neural network (De Luca et al., 2005; Fukunaga et al., 2006).

MATERIALS AND METHODS

Animal Preparations and Stimulation

A total of 10 male Sprague-Dawley rats (220–340 g) were used with experimental protocols approved by Emory University Institutional Animal Care and Use Committee. The animals were initially anesthetized with isoflurane (5% for induction and 2% during the set-up) in a mixture of O_2 and N_2 gases (3:7), delivered to the nosecone for spontaneous respiration throughout the experiment. A bolus of 0.05 mg/kg medetomidine was injected subcutaneously, and isoflurane was disconnected 10 minutes afterwards. Continuous subcutaneous infusion of medetomidine (0.1 mg/kg/hour) was started 15 minutes after the bolus injection to maintain the sedation. The head of the animal was carefully secured in the Bruker rat restrainer by using a bite bar and two flexible cushions on the two sides of the head before placement in the magnet. Rectal temperature was maintained at ~37°C by a feedback-controlled, water-circulated heating pad, and blood oxygen saturation and heart beat rate were monitored by non-invasive oxygen saturation monitor (8600V, Nonin Medical Inc., Minnesota, USA) during the preparation and fMRI experiments. The oxygen saturation was kept above 96% during the data acquisition.

For stimulation-induced fMRI study, electrical stimulation was applied to either the right or the left forepaw using two needle electrodes inserted under the skin between digits 2 and 4 and connected to a current stimulation isolator (A365D, World Precision Instruments, Inc., Sarasota, FL, USA), which was triggered by a pulse generator (Master 8, AMPI, Israel). The parameters of the electrical stimulation were adjusted for each experiment as described below.

MRI Data Acquisitions

All MRI measurements were performed on a 9.4T horizontal magnet with a bore size of 20 cm diameter, interfaced to an AVANCE console (Bruker, Billerica, MA). The gradient coil used was an actively shielded 12-cm inner diameter set with a gradient strength of 40 G/cm and a rise time of 88 μs. Two actively decoupled radio frequency (RF) coils were used: a volume coil of 7.2 cm diameter used as the transmitter, and a surface coil of 2 cm diameter positioned on the top of the animal's head as the receiver. The animal's position was adjusted based on a sagittal scout image to place the primary somatosensory cortex (SI) in the magnet center. The homogeneity of the magnetic field was optimized on a volume of $6 \times 6 \times 6$ mm^3 by using FASTMAP (Gruetter, 1993). Eight consecutive axial slices were acquired with TE=15 ms, thickness = 1 mm, matrix size = 64×64 and FOV = 3×3 cm^2, by using a multi-slices single-shot gradient echo echo-planar imaging (GE EPI). Each fMRI run consisted of 10 + **10** + 20

image acquisitions (boldface represents stimulation on) with TR = 2 s. T_1-weighted anatomical images were obtained by the MDEFT sequence with inversion preparation and an inversion time of 1.4 sec. To investigate the frequency dependence of the BOLD response, stimuli with a fixed pulse width of 0.3 ms, a current of 2 mA and varied frequencies of 1, 3, 6, 9, 12, 15 and 18 Hz were applied in an interleaved fashion in different fMRI runs. Based on the results from the frequency-dependence study, the 9 Hz stimulus led to the strongest activation in the SI (see results). Subsequently, a 9 Hz stimulus with a width of 0.3 ms was used to investigate the temporal-spatial characteristics of the activation under different stimulation strengths. Stimulus currents of 1, 2, 4, 6 and 8 mA were applied in different fMRI runs. For the stimulation studies, 10 to 20 runs under each condition were performed for signal averaging. These stimulation-induced activation fMRI experiments lasted ~3 hours. Subsequently, in 7 of the 10 rats, an additional experiment was performed without stimulation to acquire 300 volumes (10 minutes) with exactly the same imaging parameters in the same slices.

Data Analyses

Data were processed using Stimulate (Strupp, 1996) and MATLAB routines (Mathworks, Natick, MA). Stimulation-induced activation (*t* value) maps and resting-state cross correlation coefficient (CCC) maps were color-coded and overlaid on the T_1-weighted anatomical images. Graphs of mean value were plotted with standard errors of means (SEM), and results were also reported as mean ± SEM. Statistical significance was examined by one-way repeated measures ANOVA and paired t test.

With the stimulation BOLD data, *t*-value maps were computed by comparing the experimental fMRI data acquired during the control periods vs. data acquired during stimulation on a pixel-by-pixel basis and thresholded with $t > 2$ and a minimum spatial cluster size of 4 pixels ($p < 0.005$) (Forman et al., 1995). Average time courses of the 30 pixels having the top 30 *t*-values in the SI, the 10 pixels with the top *t*-values in the SII, the 20 pixels with the top *t*-values in the thalamus, and the 60 pixels with the top *t*-values in the caudate putamen (CPu) (CPu analysis for stimulation strength dependent study only) were obtained for quantitative analysis.

To determine reproducibility of stimulation-induced activation, fMRI data in stimulus strength dependence study were divided into two subsets, consisting of even and odd runs, respectively. Subsequently, activation maps were determined from each subset separately. Reproducibility of the fMRI signal changes within the ROI containing activated pixels obtained from the entire data set was assessed with correlation analysis.

With the resting-state BOLD data, pixel time courses were linearly detrended and low-pass filtered at a cutoff of 0.08 Hz (Biswal et al., 1995). Based on the stimulation-induced fMRI maps, seed regions of interest (ROI) (2×2 pixels) were selected in the SI and the thalamus, respectively. Using both the anatomical image and stimulation-induced activation map, another ROI (2×2 pixels) in the CPu and just below the activation in SI was selected as the CPu seed ROI. The average time courses from these ROIs were used as respective references and cross-correlated with all image pixels to derive corresponding connectivity maps. A correlation coefficient threshold of 0.3 and a cluster size threshold of 4 were used to threshold the functional connectivity maps ($p < 4\times10^{-6}$, taking into account the reduced degrees of freedom in the low-pass filtered data) (Forman et al., 1995; Press et al., 1992). To assess reproducibility of resting-state connectivity, a 10-minutes fMRI run without stimulation was divided into two subsets, the first 5-minutes data set and the second 5-minutes data set. Subsequently, cross correlation with the corresponding time courses from the seeds were performed on each data set individually to derive connectivity maps.

RESULTS

Stimulus frequency dependency of activation

Robust contralateral activations were detected in SI with stimulus frequencies above 1 Hz in all rats and, in each rat, the activation foci are similar under different frequencies (data not shown). Given the latter observation, data from different stimulus frequencies were averaged to improve the power of ascertaining the spatial patterns of activation. Fig. 1A shows the activation maps in four consecutive slices of the averaged data from one rat. Well-localized activations in contralateral SI and thalamus were detected and this observation is consistent for all five rats. Activation in contralateral secondary somatosensory cortex (SII) was also detected for this rat. But SII activation was only detected in three of total five rats. The incidence of activations in thalamus and SII are higher than those under the α-chloralose (Keilholz et al., 2004). In the posterior-anterior direction, activation in SI can be detected in three consecutive slices while activation in thalamus can be detected in two consecutive slices. No significant BOLD responses in the ipsilateral SI and thalamus were observed, in consistency with the previously performed BOLD fMRI studies in rats under α-chloralose (Lee et al., 2001;Silva et al., 1999) and isoflurane (Masamoto et al., 2007).

ROIs in the SI and thalamus were delineated as detailed in the method section. Figs. 1B and 1C illustrate time courses of the different frequencies in these ROIs. The 1 Hz stimulus induced a small BOLD signal change in SI and thalamus (red diamonds in Figs. 1B and 1C). The temporal profile of the BOLD response did not vary with the stimulus frequency. But the response amplitude varied significantly with the stimulus frequency. The insets show the response amplitude versus the stimulus frequency. In the SI, the highest change in the BOLD signal (1.25 ± 0.17%, n=5) was detected at 9 Hz, where the change is significantly higher than those at 1, 3 and 18 Hz, (three separate *t* test, where p values for individual *t* test were all < 0.007). The frequency preference of SI under medetomidine is similar as that under isoflurane (Masamoto et al., 2007) and is different from that (3 Hz) under α-chloralose (Silva et al., 1999). In the thalamus, the highest BOLD response (0.49 ± 0.05%, n=5) was also detected at 9 Hz. Although the response exhibits more gradual tapering off at high frequencies, the amplitude at 9 Hz is significantly higher than those at 1 and 3 Hz (two separate *t* test, where p values for individual *t* test were all < 0.01).

Stimulus strength dependency of activation

Robust contralateral SI activations were detected with all five different stimulus currents. In each rat, the activation foci did not vary with stimulus current (data not shown). Data from different currents were averaged. Fig. 2A shows the activation maps in four consecutive slices of the averaged result from one rat. In addition to activation in contralateral SI and thalamus that were detected in all five animals, contralateral SII activations were also detected in four of the five animals. Interestingly, besides the positive BOLD responses in SI, SII and thalamus, robust negative BOLD responses were detected in the Caudate Putamen (CPu) and other cortical regions of both hemispheres in all five animals.

An ROI of 30 pixels with the top *t*-values in the SI, an ROI of 10 pixels in the SII, an ROI of 20 pixels in the thalamus, and an ROI of 60 pixels in the CPu (two hemispheres) were identified. Figs. 2B, 2C, 2D and 2E illustrate the time courses in these ROIs, respectively, for the different currents. The time courses of SII have lower SNR due to its weak response and small number of activated pixels. Generally, the magnitude of BOLD response varied with the stimulus current while the temporal characteristics did not. A post-stimulus BOLD undershoot was observed in both SI and thalamus. An overshoot after stimulus-on is seen in SI and CPu, but not evident in thalamus. The time to peak is ~4 s for both positive and negative responses, consistent with the positive response under the α-chloralose (Silva and Koretsky, 2002). The

response amplitude as a function of stimulus current is plotted in the respective insets. For positive response in SI, the BOLD response monotonically increases currents above with the stimulus current until 4 mA (differences between the responses at two successive currents are statistically significant with all $p < 0.017$) and levels off at 4 mA (ANOVA: $F_{2,12} = 0.09$, $p = 0.92$). For the positive response in SII, no significance difference was observed in the BOLD response to different stimulus currents, probably due to the low SNR (ANOVA: $F_{4,15} = 1.3$, $p = 0.31$). For positive response in thalamus, the BOLD response increases monotonically with all the currents used without any leveling off (differences between the responses at two successive currents are statistically significant with all $p < 0.03$). Significant negative response was observed in the CPu for currents above 2 mA, and its magnitude increased monotonically with the stimulus current (differences between the responses at two successive currents are statistically significant with all $p < 0.015$).

In addition to consistency of activation in different animals, reproducibility was also examined. As shown in Fig. 3, activation maps corresponding to subset of even fMRI runs (Fig. 3A) are very similar to those corresponding to subset of odd fMRI runs (Fig. 3B). In the scatter-plot of activations from even subset versus those from odd subset (Fig. 3C), data of SI, SII, thalamus and CPu fall along the diagonal line, indicating that the activations are highly reproducible. Table 1 lists the correlation coefficients between the two maps averaged over all animals for the four activation regions, further demonstrating the reproducibility of activations in these regions. The data points in cortical regions with negative response are slightly scattered, but mostly lie in quadrant III, indicating consistent negative response to stimulation but with less reproducible amplitudes. For comparison, data points in a background region are also plotted in Fig. 3. This data points clearly scatter around origin, indicating random noise.

Resting-state functional connectivity and stimulation-induced neural activity

Ten-minute resting-state data were acquired in two rats of the stimulus frequency dependence study and five rats of the stimulus current dependence study. Except in one rat whose data exhibited large nonlinear baseline drift and were discarded, synchronized LFF of BOLD signal were observed in the cortices and CPu of the two hemispheres symmetrically. Consistent results were obtained in all six rats and described below. Connectivity maps in a representative rat (the same rat as shown in Fig. 2A) are shown in Fig. 4. Fig. 4A illustrates the functional connectivity maps with a seed in SI (the seed is the blue square labeled as “SI ROI”). These maps exhibit significant LFF synchronization in extended cortical regions of both hemispheres. Fig. 4B displays the functional connectivity maps with a seed in CPu (the seed is the blue square labeled as “CPu ROI”); the maps also exhibit significant LFF synchronization in CPu of both hemispheres. Compared with the stimulation-induced activity in Fig. 2A, no negative correlations were observed in regions, such as CPu, that showed significant negative BOLD response to forepaw stimulation. With the thalamus seed, no significant LFF synchronization was detected.

To demonstrate the synchronization of LFF in BOLD signal in bilateral SIs, the time course of the seed ROI in the SI in one of the hemisphere is compared with the average time course of the SI ROI in the opposite hemisphere (the ROIs are shown in Fig. 5B inset image) in Fig. 5A. Correlation between the two time courses is evident. The cross correlation coefficient between the two time courses from the bilateral SI ROIs averaged over all 6 animals is 0.53 ± 0.02 ($n = 6$, where p values for individual studies were all $< 4.9 \times 10^{-6}$). As shown in Fig. 5A, the amplitude of the synchronized LFF is ~1.5%, comparable to the stimulation-induced signal change (see Fig. 2B). The Fourier Transforms of the time courses in Fig. 5A are shown in Fig. 5B. Significant low frequency oscillations are seen in both ROIs. These low frequency peaks are also seen in the data from the other five rats.

Time courses in the bilateral CPu are also examined (the ROIs are shown in Fig. 5D inset image). As indicated in Fig. 5C, there is significant correlation between the two time courses. The inter-animal average of the cross correlation coefficient between the two time courses is 0.53 ± 0.04 (n = 6, where p values for individual studies were all $< 2 \times 10^{-4}$), demonstrating that LFF of BOLD signal in the bilateral CPu in these animals are also highly connected. The peak amplitude of the synchronized LFF in CPu is also ~1.5%. The Fourier Transforms (Fig. 5D) of the bilateral CPu time courses exhibit significant low frequency peaks. This observation is also consistent in the remaining rats.

To demonstrate the low correlation between the bilateral thalamic regions, time courses from the left and right thalami (ROIs shown in the inset image of Fig. 5F) of the same rat are presented in Fig. 5E. Unlike the time courses of SI and CPu (Fig. 5A, 5C), there are no synchronized peaks in the two thalamic time courses. The inter-animal average of the cross correlation coefficient between the time courses from the bilateral thalamic ROIs is 0.008 ± 0.04 (n = 6, where p values for individual studies were all > 0.23), indicating the absence of synchronization between the LFF of BOLD signal in the bilateral thalamus in these animals.

Although both the contralateral thalamus and contralateral SI were activated by the forepaw stimulation, no resting state connectivity was detected between them. This lack of connectivity was further supported by the comparison of the thalamic time course with that of the SI. The average of cross-correlation coefficient for all the animals is −0.04 ± 0.02 (n=6, with p values for individual studies > 0.3), which is not different from zero.

Fig. 6 shows the resting-state connectivity and stimulation-induced activation maps in the slices containing the highest stimulation-induced activation of SI for all remaining 5 rats. These maps are consistent with the maps presented in Figs. 2A and 4, exhibiting significant resting-state activations in extended cortical regions including SI and between the CPu of the two hemispheres.

Fig. 7 shows reproducibility result of the resting-state connectivity for all 6 rats. The resting-state connectivity calculated from the first half of the data (Figs. 7A, 7C) is similar to that from the second half of the data (Figs. 7B, 7D), indicating good reproducibility in the resting-state connectivity.

Discussions

Three major issues were addressed in this work. First, stimulus frequency dependence of BOLD response in rat under medetomidine was studied and found to be different from that under α-chloralose (Matsuura and Kanno, 2001; Silva et al., 1999; Ureshi et al., 2004). Of note is that the frequency “tuning curve” of thalamus response was also obtained in our study. Second, increasing the stimulation current increased the magnitudes of BOLD responses in SI, thalamus and CPu. The individual relationships are not intimately coupled. The SI response reached a plateau at a current of 4 mA while the thalamus and CPu response did not level off with increasing currents (insets of Figs. 2B, 2D and 2E). Third, BOLD studies of resting-state functional connectivity and forepaw stimulation-induced activity were performed in the same rats to compare their spatial correlation. The synchronized LFF of BOLD signals were observed between large cortical regions in two hemispheres. Interestingly, such synchronized LFF of BOLD signals were also observed in the CPu of two hemispheres. But no synchronization was found between the thalamus and the SI, which are both activated by contralateral forepaw electrical stimulation. Based on its spatial and temporal characteristics of the synchronization, it likely reflects functionally meaningful connections in the brain. The connectivity observed in this study paves the way for future studies that may elucidate the mechanisms of functional connectivity by combining more effective invasive techniques in animals.

Stimulation-induced fMRI in medetomidine-sedated rats

From frequency-dependence study, ~9 Hz frequency of the stimulus that elicited maximum BOLD response in SI under medetomidine is similar to the optimum frequency of 12 Hz under the isoflurane (Masamoto et al., 2007) and that of 10 Hz under the enflurane (Sheth et al., 2003). The 9 Hz peak frequency is significantly different from the optimum frequencies of 1–5 Hz under the α-chloralose (Detre et al., 1998; Gyngell et al., 1996; Matsuura and Kanno, 2001; Ngai et al., 1999; Nielsen and Lauritzen, 2001; Silva et al., 1999; Ureshi et al., 2004). Such a discrepancy can be caused by the different neural response and/or different neural-hemodynamic coupling under different anesthesia as suggested by Masamoto and his colleagues (Masamoto et al., 2007). Another interesting finding here is that the thalamus also shows a frequency dependence, similar to that of SI. Such finding would be helpful for the mapping of somatosensory pathway in which the thalamus is one of the important relay stations (Keilholz et al., 2004; Paxinos, 1985).

From the stimulation strength dependence study, we observed that the BOLD change in SI reached a plateau with increasing currents during forepaw stimulation (inset of Fig. 2B). This observation indicates that there is a threshold at which the maximum hemodynamic response can be induced, possibly corresponding to the maximum field potential that can be evoked by stimulation (Masamoto et al., 2007). In the present case, the parameters for BOLD to reach the plateau is 9 Hz, 0.3 ms and 4 mA. If the integration of the stimulation current represents the stimulation strength, our result (4 mA × 0.3 ms = 1.2 mA·ms to reach the plateau) is comparable to the stimulation strength under which the field potential response (8 Hz, 1 ms, 1.4 mA, 1.4 mA·ms) and CBF response (8 Hz, 1 ms, 1.6 mA, 1.6 mA·ms) reached the plateau under isoflurane (Masamoto et al., 2007). Similar stimulation strength dependence was also observed in CBF-based functional imaging and local field potential studies of current variations under α-chloralose (Nielsen and Lauritzen, 2001). Unlike the response in the SI, the BOLD response in the thalamus is smaller and do not level off even at 8 mA, suggesting the possible existence of nonlinearity in thalamocortical transmission or neuronal saturation in cortex. Since electrical activities of both the SI and the thalamus can be directly measured, an electrophysiological experiment could be performed in this animal model to study the origin of the differential responses in thalamus and cortex.

In this study, the detectability of the somatosensory pathway (thalamus, primary and secondary somatosensory cortices) under medetomidine was improved comparing with that under the α-chloralose (Keilholz et al., 2004). The stimulation-induced fMRI signal depends on the neuronal response, basal blood flow and neurovascular coupling. Anesthetics could decrease fMRI signal by suppressing neuronal response, perturbing the neurovascular coupling associated with increased neuronal activity and modulating basal blood flow (Chapin et al., 1981; Fukuda et al., 2005; Martin et al., 2006; Sicard et al., 2003). To detect fMRI signal in anesthetized animals, choice of anesthetics and level of anesthesia are important to ensure maintaining neural viability and hemodynamic response. If an anesthesia level is too high, it will substantially suppress neural activity as well as hemodynamic response to make it hard to obtain fMRI signal. In our study, the medetomidine with the suggested dose (Weber et al., 2006) was used as an anesthetic. As discussed in the next section, the rats in our study are under sedation and are far from fully anesthetized (Bol et al., 1999). Although currently there is little relevant data regarding the medetomidine effects on neuronal response, basal blood flow and neurovascular coupling with medetomidine as an independent anesthetic, it is conceivable that these physiological processes are more preserved under medetomidine with the dose used, leading to an increased detectability of the activities in the somatosensory pathway.

A robust, reproducible negative BOLD response was detected in the CPu and some cortical regions when the stimulation current is > 2mA (see Figs. 2 and 3), consistent with a recent report (Lowe et al., 2007). Since the BOLD signal is inversely proportional to the local content

of deoxyhemoglobin, the negative BOLD reflects an increase in venous blood deoxyhemoglobin, which could result from: 1) a decrease in CBF due to spatial redistribution of CBF that is independent of the local changes in neuronal activity and CMRO2 – "stealing", activated cortex stealing blood from less active regions; 2) a reduction in neuronal activity, or "deactivation", which causes the decrease in CBF exceeding the decrease in CMRO2. If it is stealing, based on fMRI study of cat visual cortex (Harel et al., 2002), negative BOLD should be mainly detected in the brain area adjacent to the positive BOLD response, and the negative BLOD amplitude should be highly correlated with the positive BOLD amplitude. Given that the negative BOLD in this study was detected in both hemispheres, distant (>5mm) from the activated site, and its amplitude in CPu is not correlated with the positive BOLD amplitude of the positive response in SI, it is not likely due to such "stealing" effect. In a BOLD and CBF study in a human visual cortex (Shmuel et al., 2002), it is shown that the region with the negative BOLD response exhibits a decrease in CBF exceeding a decrease in CMRO2 and concluded that the negative BOLD is caused by "deactivation." Furthermore, a recent study of simultaneous fMRI and electrophysiological recording of monkey visual cortex revealed a decrease in neuronal activity in the cortical region where the negative BOLD was detected and a correlation between the two and that negative BOLD region is far away (~7 mm) from the positive BOLD region (Shmuel et al., 2006). In this study, with the negative BOLD signal detected in functional related but distant regions, it is likely arising from "deactivation," which may be related with the sensation of pain (Lowe et al., 2007).

Resting-state functional connectivity in medetomidine-sedated rats

In the cortex, spatial correspondence between stimulation-induced activation and resting-state maps is observed but limited. Functional connectivity is bilateral, suggesting that resting state connectivity can identify the entire relevant network, as seen also in human subjects (De Luca et al., 2005). In the CPu, where bilateral negative BOLD response was seen during single forepaw stimulation (see Fig. 2A), a strong resting-state correlation was detected. In human studies, some regions exhibiting task-related deactivation were seen as functionally connected in the resting-state (Fox et al., 2005; Greicius et al., 2003). In summary, similar to resting state connectivity revealed in human subjects (Biswal et al., 1995; Biswal et al., 1997; Damoiseaux et al., 2006; Fukunaga et al., 2006; Greicius et al., 2003; Lowe et al., 1998), our results showed that the synchronized resting-state LFF in BOLD signal in rats under medetomidine resides in functionally networks. The ability to detect such connectivity in animals robustly paves the way for future investigation of the resting-state fMRI mechanism and opening up a new avenue of using the resting state measure in a wide range of applications that utilizes animal models.

Besides neuronal originated LFF of BOLD signal, several other physiological fluctuations may also cause fluctuation of BOLD signal. First, BOLD fluctuations caused by respiration and cardiac movements can contribute to LFF synchronization through "aliasing" effect (Biswal et al., 1996; Fukunaga et al., 2006; Lowe et al., 1998). Compared with the respiration frequency of ~1 Hz and cardiac frequency of 4–6 Hz in rats, the image sampling rate of 0.5 Hz (TR = 2 sec) in the present study is low. Such physiological fluctuations in BOLD signal cannot be identified. Due to aliasing, physiological fluctuations can alias into the low frequency range which is used for connectivity mapping. Several observations suggest that such aliased physiological noise is not the main source of the detected connection. First, the time courses and the corresponding frequency spectra of the connected ROIs shown in Fig. 5 indicate that the synchronized low frequency fluctuations do not appear to correspond to respiration which would be more periodic. Second, the temporal patterns shown in the cortical network and the CPu network are very different, indicating that they are not from a single source, such as respiration. Furthermore, as shown in Fig. 8, the connectivity patterns observed are spatially different from those of the standard deviation map of the fluctuation.

Another physiological fluctuation is from autoregulation of the cerebral vasculature (Fukunaga et al., 2006; Hudetz et al., 1992; Kiviniemi et al., 2000; Zhang et al., 1998) in response to arterial blood pressure changes which can be triggered by anesthesia (Kiviniemi et al., 2000) or in response to arterial carbon dioxide changes due to respiration (Birn et al., 2006; Wise et al., 2004) and CO_2 inhalation (Zhang et al., 1998). However, this type of BOLD fluctuations is expected to be global and exhibit two spatial characteristics. First, its magnitude should be proportional to the baseline venous blood volume hence most prominent in the cortical surface where the large veins reside (Birn et al., 2006; Cohen et al., 2004). Second, these fluctuations should reside in widespread brain regions including gray matter and white matter (Birn et al., 2006; Cohen et al., 2004; Wise et al., 2004). In the present study, correlated clusters were observed in the two hemispheres in localized regions symmetrically and distant from each other (Fig. 4 and Fig. 6B, 6C). To compare the baseline fluctuations with the connectivity maps, the functional connectivity maps (1^{st} slices in Figs. 4A and 4B) were overlaid on the baseline standard deviation (STD) map representing the baseline signal fluctuations calculated from the filtered resting-state data (Fig. 8). As expected, the baseline STD map clearly exhibits spatial differences, showing larger fluctuations near the cortical surface and midline where large draining veins reside. However, pixels with significant connectivity to the SI seed cluster in two hemispheres and do not correspond to regions with high baseline fluctuations. On the other hand, the baseline STD maps exhibit large fluctuations in CPu regions and overlap with the clusters of the significant connectivity to the seed of CPu reside, suggesting that the large fluctuations in CPu may be dominated by synchronized fluctuations. From our results, even though the contribution from the autoregulation of the cerebral vasculature could not be ruled out, the spatial pattern of our connectivity maps indicates that they reflect the neural connectivity to a good extent.

The functional connectivity detected may be specific to the medetomidine dose used in this study which retains some wakefulness in the rats during imaging. Based on the pharmacokinetic study of medetomidine in rat, its half-life in blood is ~1 hour (Bol et al., 1997). Assume that the blood volume of rat is ~5% of body weight, the blood concentration is ~1 ng/ml after the initial dose of 50 ng/kg. Subsequently, medetomidine was continuously injected at the rate of 2 ng/ml/hour. Based on pharmacokinetic analysis (Bonate, 2006), the medetomidine concentration in the blood is under 1 ng/ml during the acquisition of the resting-state fMRI data. According to a previous study (Bol et al., 1999), rats with a blood concentration of medetomidine < 1 ng/ml still have responses to whisker stoking by a pencil, cornea stoking by a paper tip, and tail clamping. Thus, the rats in our study are far from fully anesthetized. In fact, when the rats were removed from the cradle after cessation of the imaging session in this study, they were always responsive. In human subjects, functional connectivity can be detected with light anesthesia but is totally ablated with deep anesthesia (Peltier et al., 2006). Given these considerations, the functional connectivity detected in our study can be attributed to wakefulness of rat.

It is a little surprising that no thalamic connectivity and thalamocortical connection were detected in this study. The thalamus is known to be a “sensory gate” receiving afferents from sensory receptors and transferring received information to targeted cortical regions. Connectivity between thalamus and cortex is bidirectional (Killackey and Sherman, 2003). In our study, both the thalamus and the SI are activated during forepaw stimulation, verifying that the thalamus is an input relay of the somatosensory pathway. But no resting-state connectivity between thalamus and somatosensory cortex and between thalami in the two hemispheres is detected even though connectivity between bilateral somatosensory cortices was detected during resting state. It is difficult to know whether the lack of thalamocortical connection and thalamic connection in the present study is due to the anesthesia or something else. Note that a lack of functional connectivity does not mean a lack of network connection. In human studies without anesthesia, results of thalamocortical connection and thalamic connection are variable

and inconclusive. White et al. reported a positive thalamocortical connection (White and Alkire, 2006) and Goldman et al. reported a negative thalamocortical connection (Goldman et al., 2002), while no thalamocortical connection was detected by others (Fukunaga et al., 2006; Laufs et al., 2003; Moosmann et al., 2003). A thalamic connection has been reported in some studies (Fukunaga et al., 2006; Goldman et al., 2002; Laufs et al., 2003; Moosmann et al., 2003; Schreckenberger et al., 2004; Wehrle et al., 2007), but was not detected in other studies (Fukunaga et al., 2006; Laufs et al., 2003; Moosmann et al., 2003).

Based on our results, the peak amplitude of synchronized fluctuations can be as high as ~1.5% (see Figs. 5A and 5C), comparable to the amplitude of stimulation-induced fMRI signal change in this study (see Fig. 2). Since such fluctuations also act as background noise in the stimulation-induced fMRI study, they could compromise the detection of stimulus induced response. Nonetheless, their effects are minimal because they are random and their frequency content is different from that of the BOLD response to the 20-second stimuli in the present study. Furthermore, the effect of these fluctuations was significantly reduced by averaging between the repeated runs in this study.

Acknowledgements

Supported by NIH (RO1EB002009), the National Science Foundation (BES 0401627) and Georgia Research Alliance.

Reference List

Allers KA, Ruskin DN, Bergstrom DA, Freeman LE, Ghazi LJ, Tierney PL, Walters JR. Multisecond periodicities in basal ganglia firing rates correlate with theta bursts in transcortical and hippocampal EEG. J Neurophysiol 2002;87:1118–1122. [PubMed: 11826075]

Anand A, Li Y, Wang Y, Wu J, Gao S, Bukhari L, Mathews VP, Kalnin A, Lowe MJ. Antidepressant Effect on Connectivity of the Mood-Regulating Circuit: An fMRI Study. Neuropsychopharmacology 2005;30:1334–1344. [PubMed: 15856081]

Birn RM, Diamond JB, Smith MA, Bandettini PA. Separating respiratory-variation-related fluctuations from neuronal-activity-related fluctuations in fMRI. Neuroimag 2006;31:1536–1548.

Biswal B, DeYoe EA, Hyde JS. Reduction of physiological fluctuations in fMRI using digital filters. Magn Reson Med 1996;35:117–123.

Biswal B, Kylen JV, Hyde J. Simultaneous Assessment of Flow and BOLD Signals in Resting-State Functional Connectivity Maps. NMR Biomed 1997;10:165–170. [PubMed: 9430343]

Biswal B, Yetkin F, Haughton VM, Hyde J. Functional connectivity in the motor cortex of resting human brain using echo-planar MRI. Mag Reson Med 1995;34:537–541.

Bol CJJG, Danhof M, Stanski DR, Mandema JW. Pharmacokinetic-Pharmacodynamic Characterization of the Cardiovascular, Hypnotic, EEG and Ventilatory Responses to Dexmedetomidine in the Rat. J Pharmacol Exp Ther 1997;283:1051–1058. [PubMed: 9399976]

Bol CJJG, Vogelaar JPW, Mandema JW. Anesthetic profile of dexmedetomidine identified by stimulus-response and continuous measurements in rats. J Pharmacol Exp Ther 1999;291:153–160. [PubMed: 10490899]

Bonate, PL. Pharmacokinetic-Pharmacodynamic Modeling and Simulation. Spinger Science+Business Media, Inc; San Antonio: 2006.

Chapin JK, Waterhouse BD, Woodward DJ. Differences in Cutaneous Sensory Response Properties of Single Somatosensory Cortical Neurons in Awake and Halothane Anesthetized Rats. Brain Res Bull 1981;6:63–70. [PubMed: 6258757]

Cohen ER, Rostrup E, Sidaros K, Lund TE, Paulson OB, Ugurbil K, Kim SG. Hypercapnic normalization of BOLD fMRI: comparison across field strengths and pulse sequences. Neuroimag 2004;23:613–624.

Damoiseaux JS, Rombouts SARB, Barkhof F, Scheltens P, Stam CJ, Smith SM, Beckmann CF. Consistent resting-state networks across healthy subjects. Proc Natl Acad Sci USA 2006;103:13848–13853. [PubMed: 16945915]

De Luca M, Smith S, De Stefano N, Federico A, Matthews PM. Blood oxygenation level dependent contrast resting state networks are relevant to functional activity in the neocortical sensorimotor system. Exp Brain Res 2005;167:587–594. [PubMed: 16284751]

Detre JA, Ances BM, Takahashi K, Greenberg JH. Signal averaged laser Doppler measurements of activation-flow coupling in the rat forepaw somatosensory cortex. Brain Res 1998;796:91–98. [PubMed: 9689458]

Dijkhuizen RD, Singhal AB, Mandeville JB, Wu O, Halpern EF, Finklestein SP, Rosen BR, Lo EH. Correlation between Brain Reorganization, Ischemic Damage, and Neurologic Status after Transient Focal Cerebral Ischemia in Rats: A Functional Magnetic Resonance Imaging Study. J Neurosci 2003;23:510–517. [PubMed: 12533611]

Duong TQ, Silva AC, Lee SP, Kim SG. Functional MRI of Calcium-Dependent Synaptic Activity: Cross Correlation with CBF and BOLD Measurements. Magn Reson Med 2000;43:383–392. [PubMed: 10725881]

Forman SD, Cohen JD, Fitzgerald M, Eddy WF, Mintun MA, Noll DC. Improved assessment of significant activation in functional magnetic resonance imaging (fMRI): use of a cluster-size threshold. Magn Reson Med 1995;33:636–647. [PubMed: 7596267]

Fox M, Snyder AZ, Vincent JL, corbetta M, Van Essen DC, Raichle ME. The human brain is intrinsically organized into dynamic, anticorrelated functional networks. Proc Nat Acad Sci 2005;102:9673–9678. [PubMed: 15976020]

Fukuda M, Rajagopalan UM, Homma R, Matsumoto M, Nishizaki M, Tanifuji M. Localization of Activity-dependent Changes in Blood Volume to Submillimeter-scale Functional Domains in Cat Visual Cortex. Cereb Cortex 2005;15:823–833. [PubMed: 15459078]

Fukunaga M, Horovitz SG, van Gelderen P, de Zwart JA, Jansma JM, Ikonomidou VN, Chu R, Deckers RHR, Leopold DA, Duyn JH. Large-amplitude, spatially correlated fluctuations in BOLD fMRI signals during extended rest and early sleep stages. Magn Reson Imaging 2006;24:979–992. [PubMed: 16997067]

Goldman RI, Stern JM, Engel J, Cohen MS. Simultaneous EEG and fMRI of the alpha rhythm. NeuroReport 2002;13:2487–2492. [PubMed: 12499854]

Greicius MD, Krasnow B, Reiss AL, Menon V. Functional connectivity in ther resting brain: A network analysis of the default mode hypothesis. Proc Natl Acad Sci USA 2003;100:253–258. [PubMed: 12506194]

Gruetter R. Automatic, localized in vivo adjustment of all first- and second-order shim coils. Magn Reson Med 1993;29:804–811. [PubMed: 8350724]

Gyngell ML, Bock C, Schmitz B, Hoehn-Berlage M, Hossmann KA. Variation of functional MRI signal response to frequency of somatosensory stimulation in α-chloralose anesthetized rats. Magn Reson Med 1996;36:13–15. [PubMed: 8795014]

Harel N, Lee SP, Nagaoka T, Kim DS, Kim SG. Origin of negative blood oxygenation level-dependent fMRI signals. J Cereb Blood Flow and Metab 2002;22:908–917. [PubMed: 12172376]

Hudetz AG, Roman RJ, Harder DR. Spontaneous flow oscillations in the cerebral cortex during acute changes in mean arterial pressure. J Cerb Blood Flow Metabolism 1992;12:491–499.

Keilholz SD, Silva AC, Raman M, Merkle H, Koresky AP. Functional MRI of the Rodent Somatosensory Pathway Using Multislice Echo Planar Imaging. Mag Reson Med 2004;52:89–99.

Killackey HP, Sherman SM. Corticothalamic Projections from the Rat Primary Somatosensory Cortex. J Neurosci 2003;23:7381–7384. [PubMed: 12917373]

Kiviniemi V, Jauhiainen J, Tervonen O, Paakko E, Oikarinen J, Vainioipaa V, Rantala H, Biswal B. Slow vasomotor fluctuation in fMRI of anesthetized child brain. Mag Reson Med 2000;44:373–378.

Laufs H, Kleinschmidt A, Beyerle A, Eger E, Salek-Haddadi A, Preibisch C, Krakow K. EEG-correlated fMRI of human alpha activity. Neuroimag 2003;19:1463–1476.

Lee SP, Duong T, Yang G, Iadecola C, Kim SG. Relative changes of cerebral arterial and venous blood volumes during increased cerebral blood flow: Implications for BOLD fMRI. Magn Reson Med 2001;45:791–800. [PubMed: 11323805]

Lee SP, Silva AC, Kim SG. Comparison of Diffusion-weighted High-Resolution CBF and Spin-Echo BOLD fMRI at 9.4 T. Magn Reson Med 2002;47:736–741. [PubMed: 11948735]

Leopold DA, Murayama Y, Logothetis NK. Very slow activity fluctuations in monkey visual cortex: implications for functional brain imaging. Cereb Cortex 2003;13:422–433. [PubMed: 12631571]

Li S, Biswal B, Li Z, Risinger R, Rainey C, Cho J, Salmeron BJ, Stein EA. Cocaine Administration Decreases Functional Connectivity in Human Primary Visual and Motor Cortex as Detected by Functional MRI. Mag Reson Med 2000;43:45–51.

Li S, Li Z, Wu G, Zhang M, Franczak M, Antuono PG. Alzheimer Disease: Evaluation of a Functional MR Imaging Index as a Marker. Radiology 2002;225:253–259. [PubMed: 12355013]

Logothetis NK, Pauls J, Augath M, Trinath T, Oeltermann A. Neurophysiological investigation of the basis of the fMRI signal. Nature 2001;412:150–157. [PubMed: 11449264]

Lowe AS, Beech JS, Williams SCR. Small animal, whole brain fMRI: innocuous and nociceptive forepaw stimulation. Neuroimag. 2007In Press

Lowe MJ, Mock BJ, Sorenson JA. Functional Connectivity in Single and Multislice Echoplanar Imaging Using Resting-State Fluctuations. NeuroImage 1998;7:119–132. [PubMed: 9558644]

Lowe MJ, Phillips MD, Mattson D, Dzemidzic M, Matthews VP. Multiple sclerosis: low-frequency temporal blood oxygen level-dependent fluctuations indicate reduced functional connectivity - initial results. Radiology 2002;224:184–192. [PubMed: 12091681]

Lukasik VM, Gillies RJ. Animal anaesthesia for in vivo magnetic resonance. NMR Biomed 2003;16:459–467. [PubMed: 14696002]

Martin C, Martindale J, Berwick J, Mayhew J. Investigating neural-hemodynamic coupling and the hemodynamic response function in the awake rat. NeuroImage 2006;32:33–48. [PubMed: 16725349]

Masamoto K, Kim T, Fukuda M, Wang P, Kim SG. Relationship between neural, vascular, and BOLD signals in Isoflurane-anesthetized rat somatosensory cortex. Cereb Cortex 2007;17:942–950. [PubMed: 16731882]

Matsuura T, Kanno I. Quantitative and temporal relationship between local cerebral blood flow and neuronal activation induced by somatosensory stimulation in rats. Neurosci Res 2001;40:281–290. [PubMed: 11448520]

Moosmann M, Ritter P, Krastel I, Brink A, Thees S, Blankenburg F, Taskin B, Obrig H, Villringer A. Correlates of alpha rhythm in functional magnetic resonance imaging and near infrared spectroscopy. Neuroimag 2003;20:145–158.

Ngai AC, Jolley MA, D'Ambrosio R, Meno JR, Winn HR. Frequency-dependent changes in cerebral blood flow and evoked potentials during somatosensory stimulation in the rat. Brain Res 1999;837:221–228. [PubMed: 10434006]

Nielsen AN, Lauritzen M. Coupling and uncoupling of activity-dependent increase of neuronal activity and blood flow in rat somatosensory cortex. J Physiol 2001;533:773–785. [PubMed: 11410634]

Ogawa S, Lee TM. Magnetic Resonance Imaging of Blood Vessels at High Fields: in Vivo and in Vitro Measurments and Image Simulation. Magn Reson Med 1990;16:9–18. [PubMed: 2255240]

Ogawa S, Lee TM, Nayak AS, Glynn P. Oxygenation-sensitive contrast in magnetic resonance image of rodent brain at high magnetic fields. Magn Reson Med 1990;14:68–78. [PubMed: 2161986]

Ogawa S, Lee TM, Stepnoski R, Chen W, Zhu XH, Ugurbil K. An approach to probe some neural systems interaction by functional MRI at neural time scale down to milliseconds. Proc Natl Acad Sci USA 2000;97:11026–11031. [PubMed: 11005873]

Ogawa S, Menon RS, Tank DW, Kim SG, Merkle H, Ellermann JM, Ugurbil K. Functional Brain Mapping by Blood Oxygenation Level-Dependent Contrast Magnetic Resonance Imaging. Biophys J 1993;64:800–812.

Paxinos, G. The Rat Nervous System. Academic Press; 1985.

Peltier SJ, Kerssens C, Hamann SB, Sebel PS, Byas-Smith M, Hu X. Functional connectivity changes with concentration of sevoflurane anesthesia. NeuroReport 2006;16:285–288. [PubMed: 15706237]

Press, WH.; Teukolsky, SA.; Vetterling, WT.; Flannery, BP. Statistical Description of Data. In: Press, WH.; Teukolsky, SA.; Vetterling, WT.; Flannery, BP., editors. Numerical recipes. C. Cambridge University Press; Cambridge: 1992. p. 503-506.

Ruskin DN, Bergstrom DA, kaneoke Y, Patel BN, Twery MJ, Walters JR. Multisecond oscillations in firing rate in the basal ganglia: robust modulation by dopamine receptor activation and anesthesia. J Neurophysiol 1999;81:2046–2055. [PubMed: 10322046]

Ruskin DN, Bergstrom DA, Tierney PL, Walters JR. Correlated multisecond oscillations in firing rate in the basal ganglia: modulation by dopamine and the subthalamic nucleus. Neurosci 2003;117:427–438.

Schreckenberger M, Lange-Asschenfeld C, Lochmann M, Mann K, Siessmeier T, Buchholz H, Bartenstein P, Grunder G. The thalamus as the generator and modulator of EEG alpha rhythm: a combined PET/EEG study with lorazepam challenge in humans. Neuroimag 2004;22:637–644.

Sheth S, Nemoto M, Guiou M, Walker M, Pouratian N, Toga AW. Evaluation of coupling between optical intrinsic signals and neuronal activity in rat somatosensory cortex. NeuroImage 2003;19:884–894. [PubMed: 12880817]

Sheth SA, Nemoto M, Guiou M, Walker M, Toga AW. Spatiotemporal evolution of functional hemodynamic changes and their relationship to neuronal activity. J Cereb Blood Flow Metab 2005;25:830–841. [PubMed: 15744249]

Shmuel A, Augath M, Oeltermann A, Logothetis NK. Negative functional MRI response correlates with decreases in neuronal activity in monkey visual area V1. Nat Neurosci 2006;9:569–577. [PubMed: 16547508]

Shmuel A, Yacoub E, Pfeuffer J, Van De Moortele P, Adriany G, Hu X, Ugurbil K. Sustained Negative BOLD, Blood Flow and Oxygen Consumption Response and Its Coupling to the Positive Response in the Human Brain. Neuron 2002;36:1195–1210. [PubMed: 12495632]

Sicard K, Shen Q, Brevard ME, Sullivan R, Ferris CF, King JA, Duong TQ. Regional Cerebral Blood Flow and BOLD Responses in Conscious and Anesthetized Rats Under Basal and Hypercapnic Conditions: Implications for Functional MRI Studies. J Cereb Blood Flow & Metab 2003;23:472–481. [PubMed: 12679724]

Silva AC, Koretsky AP. Laminar specificity of fMRI onset times during somatosensory stimulation in rat. Proc Natl Acad Sci USA 2002;99:15182–15187. [PubMed: 12407177]

Silva A, Lee SP, Yang C, Iadecola C, Kim SG. Simultaneous blood oxygenation level-dependent and cerebral blood flow functional magnetic resonance imaging during forepaw stimulation in the rat. J Cereb Blood Flow Metab 1999;19:871–879. [PubMed: 10458594]

Stein T, Moritz C, Quigley M, Cordes D, Haughton V, Meyerand E. Functional Connectivity in the Thalamus and Hippocampus Studied with Functional MR Imaging. Am J Neuroradiol 2000;21:1397–1401. [PubMed: 11003270]

Ureshi M, Matsuura bT, Kannoa I. Stimulus frequency dependence of the linear relationship between local cerebral blood flow and field potential evoked by activation of rat somatosensory cortex. Neurosci Res 2004;48:147–153. [PubMed: 14741389]

Weber R, Ramos-Cabrer P, Weidermann D, van Camp N, Hoehn M. A fully noninvasive and robust experimental protocol for longitudinal fMRI studies in the rat. Neuroimag 2006;29:1303–1310.

Wehrle R, Kaufmann L, Wetter TC, Holsboer F, Auer DP, Pollmacher T, Czisch M. Functional Microstates within Human REM Sleep: First Evidence from fMRI of a Thalamocortical Network Specific for Phasic REM Periods. Eur J Neurosci 2007;25:863–871. [PubMed: 17328781]

White NS, Alkire MT. Impaired thalamocortical connectivity in humans during general-anesthetic-induced unconsciousness. NeuroImage 2006;19:402–411. [PubMed: 12814589]

Wise RG, Ide K, Poulin MJ, Tracey I. Resting fluctuations in arterial carbon dioxide induce significant low frequency variations in BOLD signal. Neuroimag 2004;21:1652–1664.

Zhang R, Zuckerman JH, Giller CA, Levine BD. Transfer function analysis of dynamic cerebral autoregulation in humans. Am J Physiol 1998:H233–H241. [PubMed: 9458872]

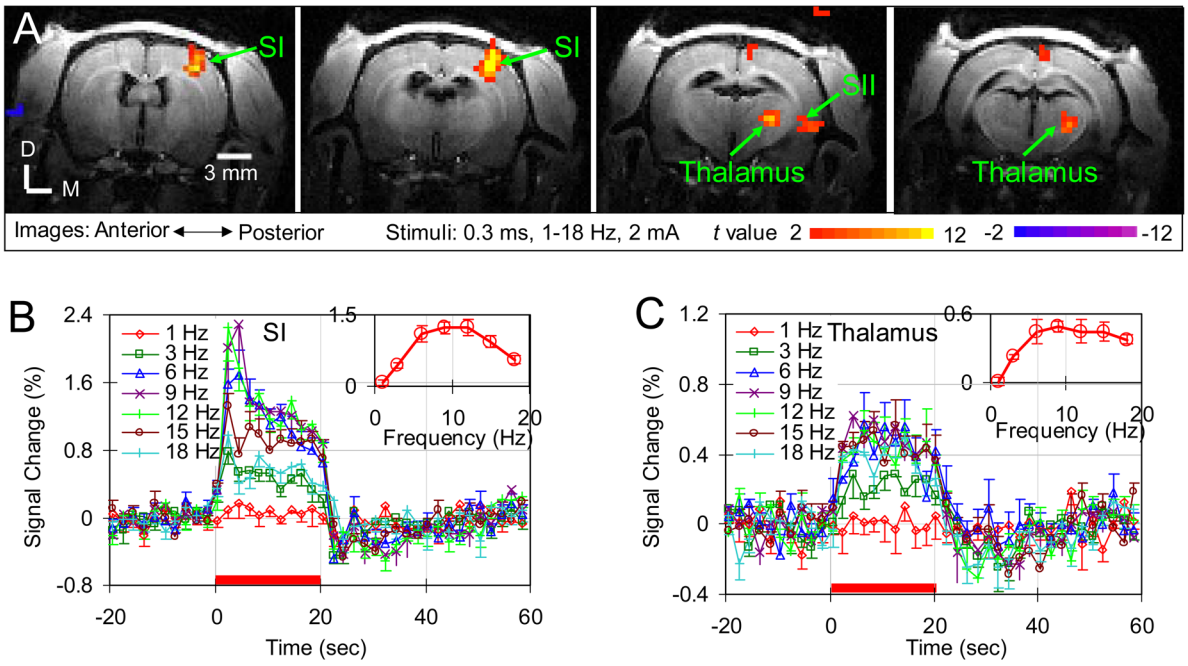

Fig. 1. Stimulus frequency dependence of BOLD response in medetomidine-sedated rats

(**A**) Left forepaw electrical stimulation-induced BOLD response of one animal in four consecutive slices (slice thickness: 1 mm) are displayed as *t*-value maps on corresponding T_1-weighted anatomical images. Positive BOLD responses (red/yellow) are observed in contralateral forepaw areas of the primary and secondary somatosensory cortices (SI and SII), as well as in contralateral thalamus. D: Dorsal; M: Medial. (**B**) Averaged time courses within the SI and (**C**) thalamus of five animals are plotted for seven different stimulus frequencies (mean ± SEM, n=5). Red bars under the time courses indicate the 20 sec stimulation period. The insets show the response amplitude versus the stimulus frequency.

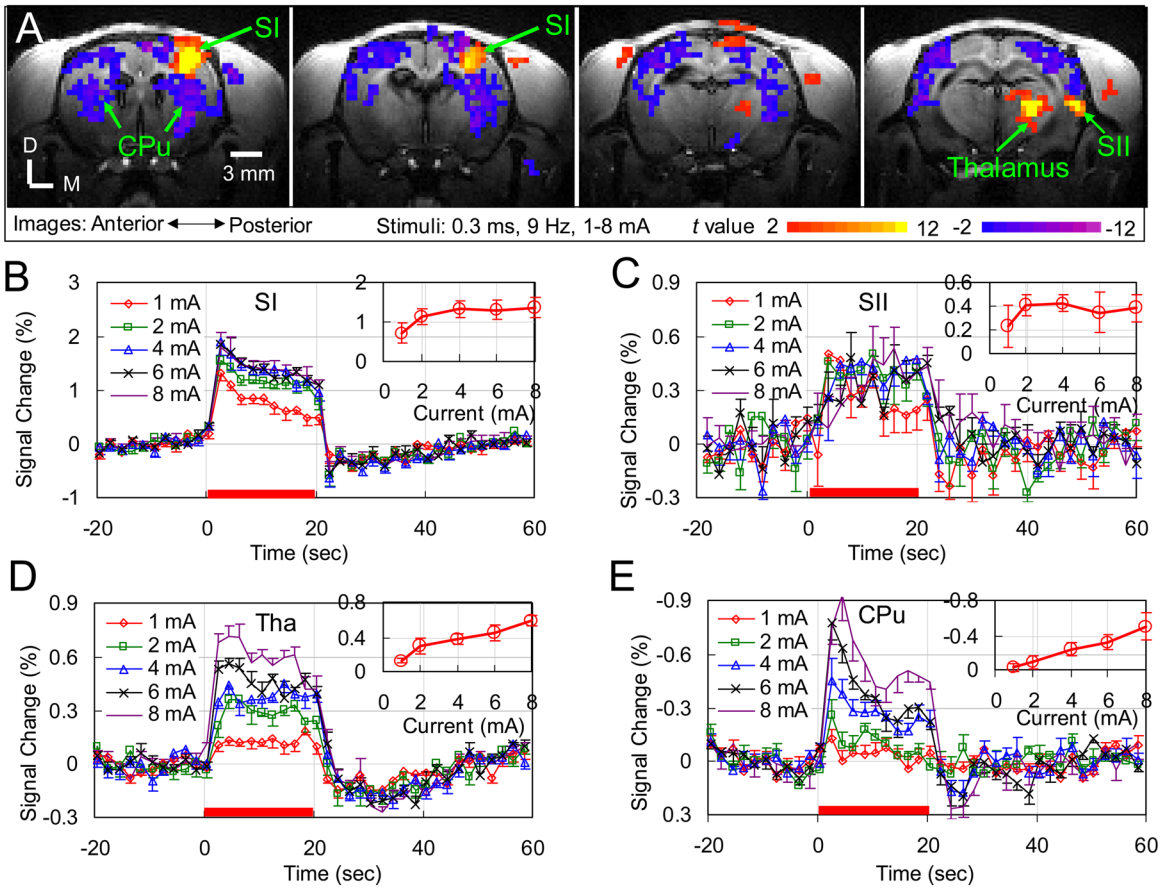

Fig. 2. Stimulus strength dependence of BOLD response in medetomidine-sedated rats

(**A**) Left forepaw electrical stimulation-induced BOLD response of one animal in four consecutive slices (slice thickness: 1 mm) are displayed as *t*-value maps on corresponding T_1-weighted anatomical images. Positive BOLD responses (red/yellow) are observed in contralateral forepaw areas of the primary and secondary somatosensory cortices (SI and SII) and thalamus, while negative BOLD responses (blue/violet) are observed in the bilateral Caudate Putamens (CPu) and other cortical regions of both hemispheres. D: Dorsal; M: Medial. (**B**) Averaged time courses within the SI, (**C**) SII, (**D**) Thalamus, and (**E**) CPu of five animals are plotted for five different stimulus currents (mean ± SEM, n=5). Red bars under the time courses indicate the 20 sec stimulation period. The insets show the response amplitude versus the stimulus current.

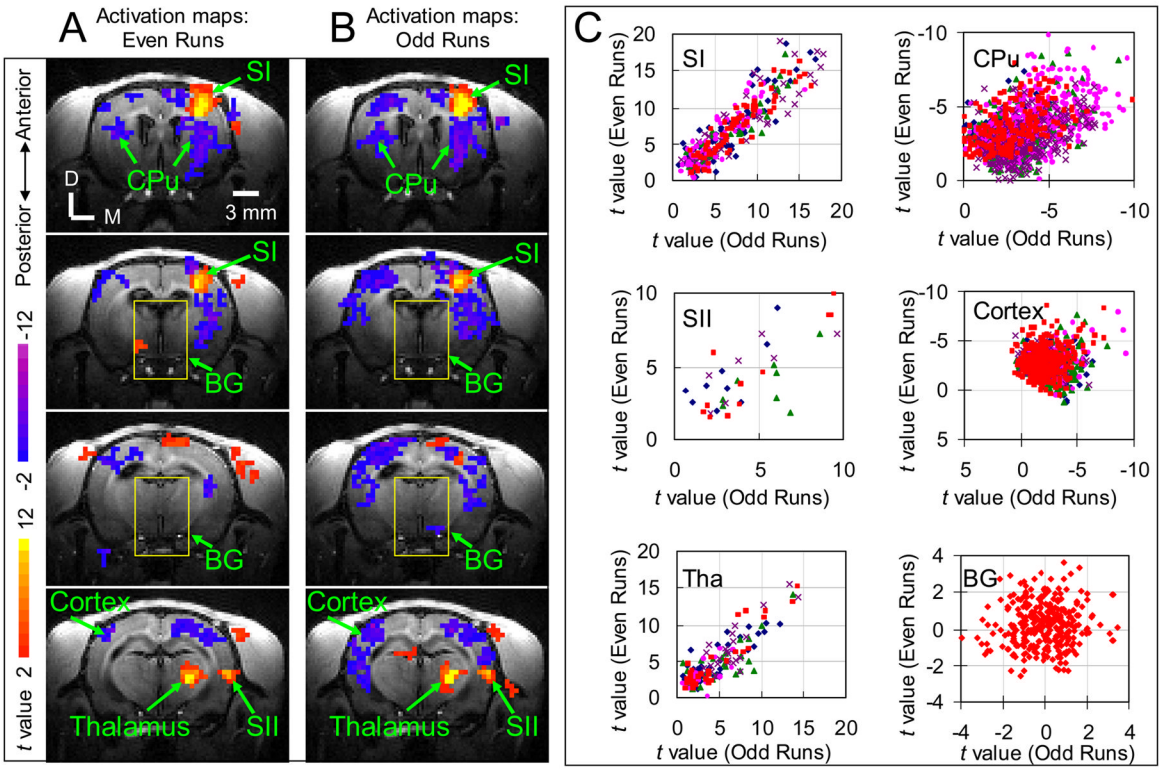

Fig. 3. Reproducibility of stimulation-induced activations

fMRI measurements of stimulus strength dependence study were divided into two sub-groups, consisting of either even or odd runs. From these subsets, separate activation maps were derived and shown in (**A**) and (**B**). The t values within the ROIs (indicated by arrows) of activated regions and backgrounds (BG, as in yellow box) for two subsets are plotted against each other in (**C**) with red data points representing the data from the animal shown in (**A**) and (**B**) and other color data points showing data from the remaining animals (one color corresponds to one animal). For the red data points, the cross correlation values are 0.93 ($p = 1.5 \times 10^{-41}$) for SI, 0.9 ($p = 3.4 \times 10^{-6}$) for SII, 0.93 ($p = 5.6 \times 10^{-21}$) for thalamus, 0.48 ($p = 9.0 \times 10^{-13}$) for CPu, 0.17 ($p = 1.3 \times 10^{-3}$) for cortical regions with negative response, and 0.06 ($p = 0.3$) for background regions. D: Dorsal; M: Medial. Cortex: cortical regions with negative response. BG: background regions as indicated by yellow boxes in (**A**) and (**B**).

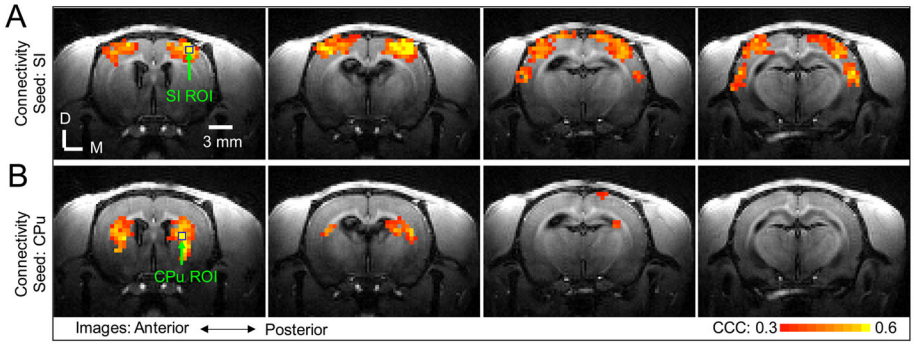

Fig. 4. Resting-state connectivity in medetomidine-sedated rats

The resting-state connectivity in four consecutive slices (slice thickness: 1 mm) from the same animal presented in Fig 2A is displayed as cross-correlation coefficient (CCC) maps calculated by correlating the time course of pixels with the time course of the seed in SI (**A**) and with the time course of the seed in CPu (**B**). The seed pixels in SI and CPu are marked by blue squares. Significant pixels were thresholded at CCC > 0.3 and spatial cluster size > 4 ($p < 4\times10^{-6}$**).** D: Dorsal; M: Medial.

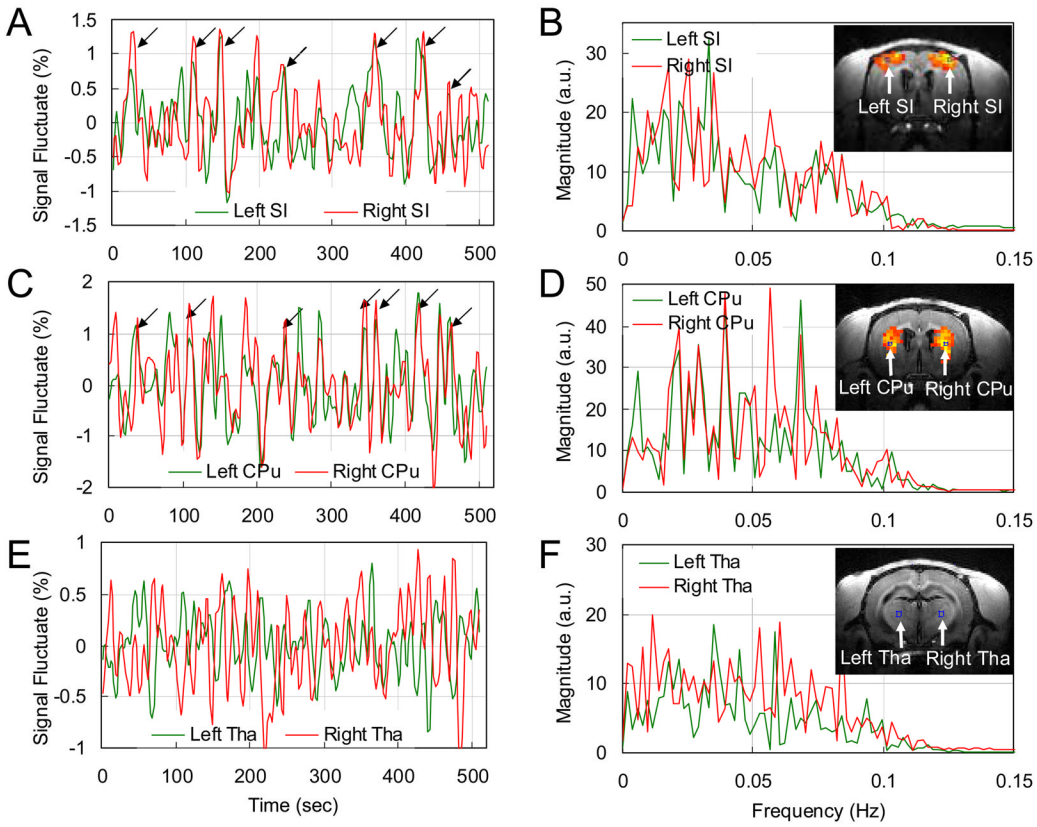

Fig. 5. Comparisons of the time courses from symmetrical ROIs of two hemispheres during resting-state and their Fourier Transforms

The time courses from left side (green) and right side (red) ROIs of SI (**A**), CPu (**C**) and thalamus (**E**) are displayed as percentage signal fluctuate. The ROIs are indicated on the inset in resting-state connectivity maps of (**B**), (**D**) and (**F**), respectively. Synchronized peaks are observed in the time courses of the SI and the CPu as indicated by black arrows in (**A**) and (**C**), while no such synchronized peaks are observed in the time courses of the thalamic ROIs (**E**). The cross correlation coefficient between the two time courses in (**A**) is 0.56 ($p = 2 \times 10^{-9}$), in (**C**) is 0.63 ($p = 4 \times 10^{-12}$) and in (**E**) is −0.03 ($p = 0.78$). (**B**), (**D**) and (**F**) are Fourier Transforms of (**A**), (**C**) and (**E**), respectively. Significant low frequency peaks are observed in (**B**) and (**D**), not evident in (**F**). Note that inset images of (**B**) and (**D**) are different from that of (**F**). Tha: thalamus.

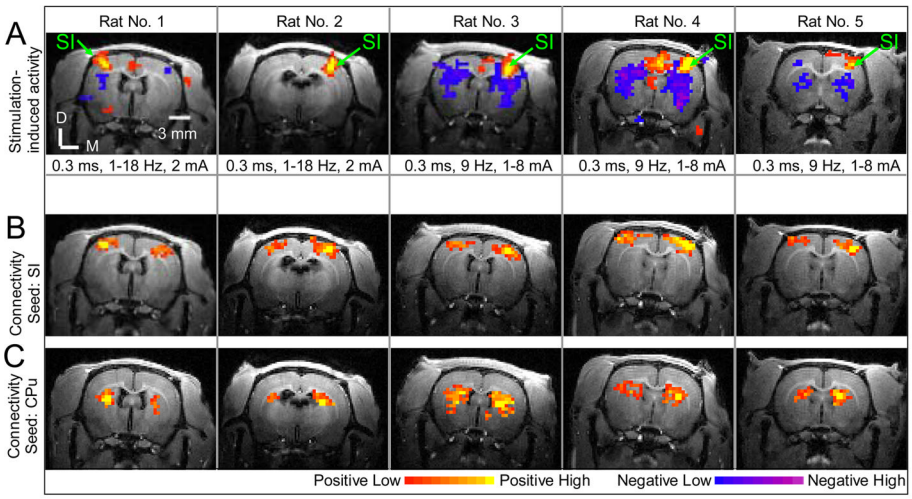

Fig. 6. Stimulation-induced neural activation and resting-state connectivity of five animals in the slices where the primary somatosensory cortices reside

(A) presents the stimulation-induced activation maps. The significant positive signal changes (red/yellow) were observed in contralateral forepaw area of the primary somatosensory cortex (SI). The stimulus parameters were listed under the stimulation-induced activation maps, respectively. (**B**) shows the corresponding resting-state connectivity maps with the seed in SI. Significant connectivity is observed in bilateral cortices for all five animals. (**C**) displays the corresponding resting-state connectivity maps with the seed in CPu. Significant connectivity is observed in bilateral CPu. The color bars for (**A**) are t-values: 2 (−2) to 12 (−12) for positive (negative) responses, respectively. The color bars for (**B**) and (**C**) are cross correlation coefficients (CCC): 0.3 to 0.6 for positive correlation. D: Dorsal; M: Medial.

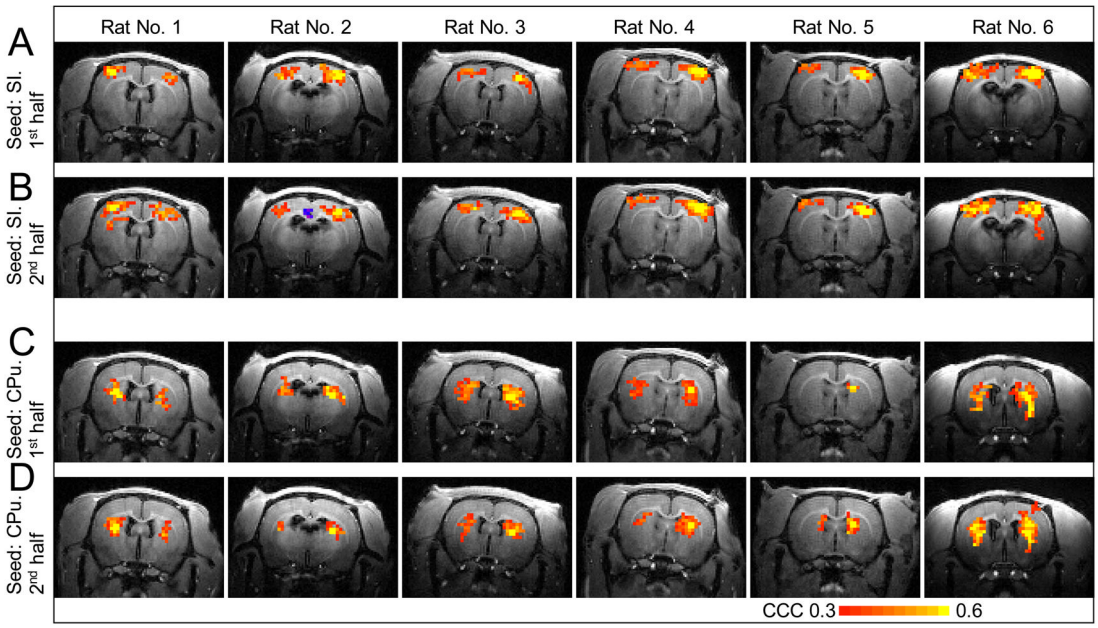

Fig. 7. Reproducibility of resting-state connectivity

A 10-minutes fMRI run without stimulation was divided into two 5-minutes subsets. From these subsets, cross-correlation coefficient (CCC) maps were calculated by correlating the time course of pixels with the time course of the seed in SI (**A, B**) and with the time course of the seed in CPu (**C, D**). Rats 1–5 correspond to those shown in Fig. 6 and rat 6 is the one whose data is displayed in Fig. 4.

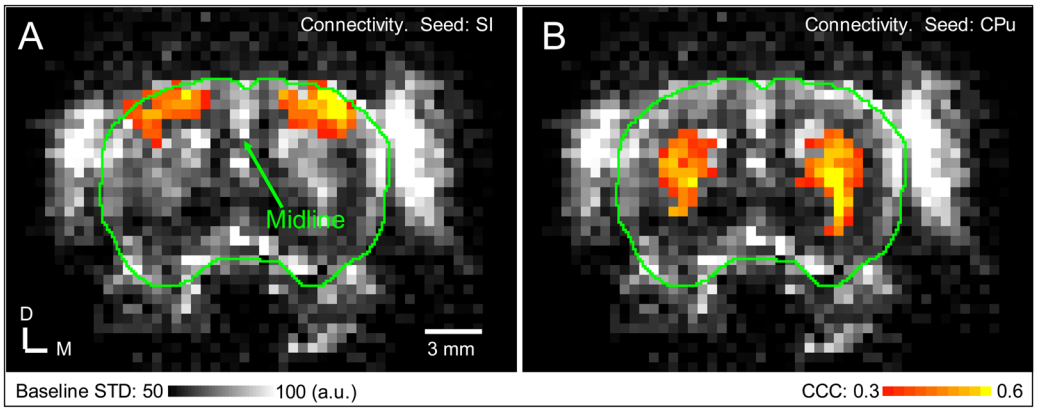

Fig. 8. Relation between resting-state connectivity and baseline signal fluctuation

Resting-state connectivity maps of SI (**A**) and CPu (**B**) were overlaid on the baseline standard deviation (STD) map. Green contour outlining the cortical surface from T1-weighted image was overlaid on the baseline STD map. Data from the first slice shown in Fig. 4 is shown. D: Dorsal; M: Medial.

Table 1

Reproducibility of activations in different regions.

	SI	SII[1]	Thalamus	CPu
CC[2]	0.90 ± 0.02	0.76 ± 0.13	0.81 ± 0.10	0.42 ± 0.13
P-value[3]	8.8×10^{-27}	0.08	0.002	0.01
Pixels[4]	64 ± 11	10 ± 2	30 ± 9	276 ± 137

[1] SII activation is only observed in 4 rats, while other activations are observed in all five rats.

[2] CC is averaged correlation coefficient between the two maps obtained from two data subsets for all animals.

[3] *P*-value is the maximum *P*-value for all animals.

[4] Pixels is averaged activated pixels for all animals.